

Simulation methodology for dielectrophoresis in microelectronic Lab-on-a-chip

A. Leonardi[†], G. Medoro[‡], N. Manaresi[‡], M. Tartagni[†] and R. Guerrieri[†]

[†]ARCES - University of Bologna, Bologna, Italy Viale Risorgimento, 2 I-40136 Bologna, Italy

Tel: +39-051-209-3557, Fax: +39-051-209-3073/3779

{aleonardi,mtartagni,rguerrieri}@deis.unibo.it

[‡]Silicon Biosystems s.r.l., Via Rialto, 31 I-40124 Bologna, Italy

{gmedoro,nmanaresi}@siliconbiosystems.com

ABSTRACT

Recent trends in lab-on-a-chip show a growing use of dielectrophoresis (DEP) to manipulate biological objects such as cells and organic molecules [1], [2], [3], [4]. Bringing the advances of microelectronic miniaturization into biological and clinical analyses, combinatorial chemistry and high throughput screening require new simulation tools. Dielectrophoretic simulators have been presented in the literature based on simplifying assumptions [5]. This paper presents a simulation methodology able to determine DEP forces on particles of arbitrary complex geometries and size, permitting accurate modeling of their position, overcoming the limitations of previous simulators. Simulation results are obtained using a 2D version of the simulator based on the developed 3D theory.

Keywords: Biosensors, Actuators, Dielectrophoresis, Microelectronics, E.M. Fields.

1 STATE OF THE ART IN DEP MODELING

Dielectrophoresis is the physical phenomenon whereby neutral particles, when subject to a nonuniform, time stationary (DC) or time varying (AC) electric field \vec{E} , experience a net force directed towards locations with increasing or decreasing field intensity according to the polarization properties of the matter. DEP force calculation, however, is a difficult task unless simplifying assumptions and simple geometries are taken into account. Many theoretical and experimental works in dielectrophoresis have used the force expression introduced by Pohl [6]:

$$\vec{F} = (\vec{p} \cdot \vec{\nabla}) \vec{E}, \quad (1)$$

where \vec{p} is the dipole moment and \vec{E} is the electric field. In order to obtain the DEP force for a spherical particle a \vec{p}_{eff} must be introduced to take into account particle geometry. This is reasonable under a first-order dipole approximation, which holds only if the radius r of particles is very small compared to electrode-system

spatial features (l electrode width). The force can be computed in closed form for simple particle geometries like spheres, shelled spheres or ellipsoid. A natural extension of analysis given by (1) allows to calculate the time-averaged DEP force exerted on a dielectric sphere immersed in a normal medium and subject to sinusoidal electric field generated by in-phase and counter-phase voltage signal as:

$$\langle \vec{F}(t) \rangle = 2\pi\epsilon_0\epsilon_m R^3 \text{Re}[f_{CM}] \vec{\nabla} (E_{RMS})^2, \quad (2)$$

where ϵ_0 is the vacuum dielectric constant, r is the particle radius, E_{RMS} is the root mean square value of the electric field, and f_{CM} is the Clausius-Mossotti factor, a complex function of the medium and particle electric permittivities [7]. Its real part is given by:

$$\text{Re}[f_{CM}] = \frac{\epsilon_p - \epsilon_m}{\epsilon_p + 2\epsilon_m}.$$

As shown by equation (2), a DEP force can be determined as the gradient of a dielectrophoretic potential where particles are pushed towards its minima and DEP forces are equal to zero. Use of equation (2) for DEP force calculation has serious drawbacks. Microelectronic miniaturization allows to implement electrodes generating electric field into lab-on-a-chip and whose dimensions are comparable with particle radius. In this case, the first-order dipole approximation can not be employed, since the dielectrophoretic potential determined by using equation (2) is not correct unless $r \ll l$ becoming a cause of error in the determination of particle position and motion.

2 OUR IMPROVEMENT

Under the hypotheses (often verified in practice) that $\epsilon \gg \sigma/\omega$, and that in-phase and counter-phase voltages generate electric field as above, the system can be considered conservative. We propose to exploit the principle of virtual works to calculate forces acting on particles by differentiating the system potential energy [8]. For a generic system made up of n conductors immersed in a normal medium, the force acting on the system is given by:

$$\vec{F} = -\vec{\nabla} U,$$

where the electrostatic energy of the system U , under the hypothesis mentioned before, can be written as:

$$U = \frac{1}{2} \sum_{h=1}^N \sum_{k=1}^N v_h v_k C_{hk},$$

where v_h and v_k are the sinusoidal potential applied to electrodes h and k respectively, and C_{hk} is the related capacitance. Elements C_{hk} can easily be computed by using a Laplace equation solver, like those employed in device modeling [9]. The time-averaged equation is given by:

$$\langle \vec{F}(t) \rangle = \frac{1}{4} \sum_{h=1}^N \sum_{k=1}^N V_h V_k \vec{\nabla} C_{hk}, \quad (3)$$

where V_h and V_k are the amplitudes of a sinusoidal potential applied to electrodes h and k respectively, and C_{hk} is the related capacitance. As shown in fig.1, the DEP force acting along the Δp displacement is numerically computed by taking the difference in capacitances with the particle at positions p and $p + \Delta p$, respectively.

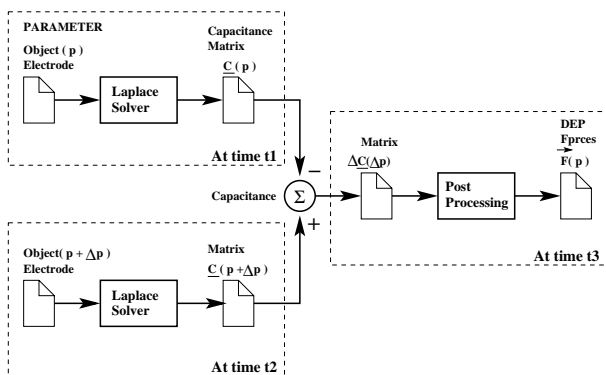


Figure 1: Simulation data flow for DEP forces evaluation in only one point of the space.

The simulation data flow described in fig.1 allows to evaluate DEP forces acting in only one point. If we want to evaluate DEP forces along a specific cross section or surface we have to map the cross section or the surface as a grid of points and evaluate DEP forces for each node. The advantages of using this approach are here summarized:

1. DEP forces can be calculated with respect to any shape of the object;
2. simulations are NOT limited to first order approximations as implied by using eq. (2).

2.1 Simulations Approximation

To investigate the performance of the methodology, we simulated DEP force in a microelectronic structure able to manipulate cells and microbeads by means of dielectrophoresis, as illustrated in fig.2.

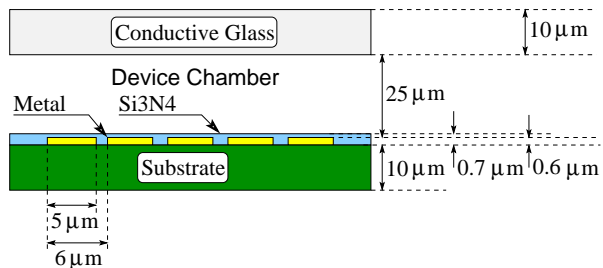


Figure 2: Simplified structure of microelectronic device implementing DEP cages.

In this case we use a 2D version of the simulator based on the general 3D equation (3). We take in account this approximation in order to reduce the computing time that becomes very high making more difficult an exhaustive investigation of our methodology. After having defined the nodes in the cross section or surface along which we want to evaluate DEP forces, DEP forces calculation must be carried out for any of them. According to the dimensions of the cross section or the surface and the accuracy of the map, we typically have a number of nodes between 20 and 100. The computing time to evaluate DEP forces for a single node of the grid is an important performance parameter. In order to characterize the performance of the simulator, tab.1 shows the computing time for evaluating DEP forces in one point of the grid for both 3D and 2D structures of fig.2. The computing time for 2D simulations is one order of magnitude smaller than 3D ones.

2.2 2D Simulations

The 2D DEP simulator determines DEP forces per unit length, while equation (2) gives DEP forces acting on a sphere. To compare these two methodologies we solve the Laplace equation for the cylindrical case considering an infinite long cylinder, obtaining a DEP forces per unit length. Solving the Laplace equation for a cylindrical rod of infinite length and cross section $S = \pi R^2$, immersed in a uniform and parallel electric

Table 1: Computing performance of the simulator. Table describes the time employed to evaluate DEP forces in only one point of the microchamber according the accuracy of the Laplace solver grid indicated by nodes number.

Computer		
Pentium III - 800 MHz		
RAM 1 Gb		
Structure	Number of nodes	Computing time
2D	10 000	30''
2D	20 000	1'
3D	100 000	10'
3D	500 000	20' - 30'

field E_0 we obtain the following equation system [11]:

$$\begin{cases} r \frac{d}{dr} r \frac{dF_1(r)}{dr} = KF_1(r) \\ \frac{d^2 F_2(\theta)}{d\theta^2} + KF_2(\theta) = 0 \\ \frac{dF_3(z)}{dz} = 0 \end{cases}$$

where K is a constant, the electrical potential is $\Phi = F_1(r)F_2(\theta)F_3(z)$, and $\{r, \theta, z\}$ are the cylindrical coordinates. If the field intensity at the surface of the cylinder remains finite, then Φ_m must become identical with Φ_p at this boundary, where Φ_m and Φ_p are respectively the electric field inside the suspending medium and the particle. If we consider an uncharged particle the normal component of $\vec{D} = \epsilon \vec{E}$ must be continuous. Hence at $r = R$, where R is the rod radius,

$$\begin{aligned} \Phi_m &= \Phi_p; \\ \epsilon_m \frac{d\Phi_m}{dr} &= \epsilon_p \frac{d\Phi_p}{dr}. \end{aligned}$$

Far from the cylinder, the field is not perturbed, hence

$$\Phi_m = -\vec{E}_0 r \cos(\theta) = -\vec{E}_0 x.$$

Solving this differential system we can evaluate the polarization \vec{P} and the moment dipole acting on the cylinder. In an inhomogeneous field \vec{E} a translational force acts on the cylinder is:

$$\vec{F}(t) = \vec{\mu} \cdot \vec{\nabla} \vec{E} = \pi \epsilon_0 \epsilon_m R^2 \frac{\epsilon_p - \epsilon_m}{\epsilon_p + \epsilon_m} \vec{\nabla} (E)^2,$$

where $\vec{\mu}$ is the dipole moment given by:

$$\vec{\mu} = \vec{P}V,$$

where \vec{P} is the polarization (constant and parallel inside the rod as result of previous analysis and shown

in fig. 3) and V is the volume [10]. Thus, by using sinusoidal signals excitation, the time-averaged DEP forces per unit length can be calculated [7] as

$$\langle \vec{F}(t) \rangle = \pi \epsilon_0 \epsilon_m R^2 \frac{\epsilon_p - \epsilon_m}{\epsilon_p + \epsilon_m} \vec{\nabla} (E_{RMS})^2, \quad (4)$$

which is similar to equation (2). Equation (2) can be compared with (4) to evaluate on the same geometry higher-order effects that are included in our approach.

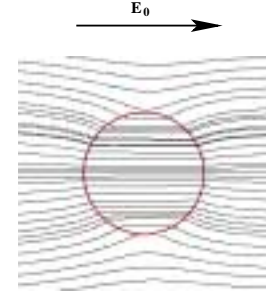


Figure 3: Dielectric cylinder in homogeneous field. The figure shows the distribution of the electric field flow lines.

3 SIMULATION RESULTS

To investigate the performance of the methodology, we computed DEP forces in a microelectronic structure able to manipulate cells and microbeads by means of dielectrophoresis, as illustrated in fig.2 [3]. In this case, the cage height for particles of different radii is plotted in fig.4 using both equation (3) and equation (4).

It is apparent that the difference between the cage height calculated using these equations increases with the particle radius because higher-order moments, neglected in (4), become increasingly important. Another important result emerging from simulations is illustrated in figures 5 and 6, where the vertical and horizontal DEP force is plotted for different radii. The maximum value of the DEP force is obtained when $R = l$. This result

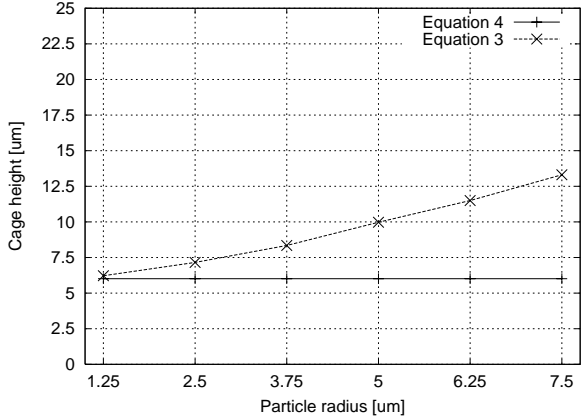


Figure 4: Comparison between simulated DEP cage height using equation (2) and equation (3), assuming, as reference, the structure shown in fig.2, potential amplitude of 1.25V and different values of the particle radius.

is of great importance for designers to optimize lab-on-a-chip geometries. As an example of accuracy of our approach, if we use equation (4) for trapping height calculation we commit a 20% average error as shown in fig.4.

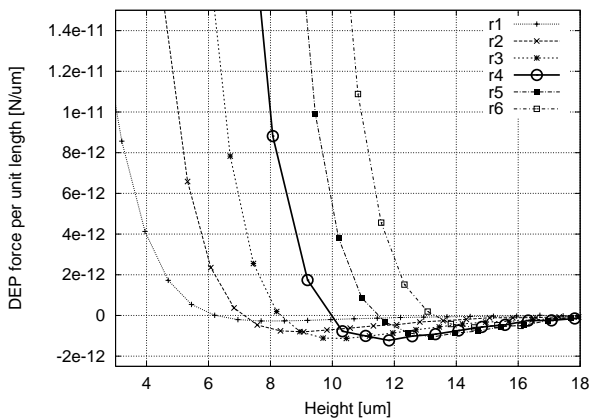


Figure 5: DEP forces magnitude per unit length along a vertical cross-section including cage center, plotted under the same hypothesis as fig.4. Radius values: $r_1 = 1.25 \mu m$, $r_2 = 2.5 \mu m$, $r_3 = 3.75 \mu m$, $r_4 = 5 \mu m$, $r_5 = 6.25 \mu m$, $r_6 = 7.5 \mu m$. The highest DEP force is obtained when $R = l$, where R is the cylinder radius and l is the electrode width.

REFERENCES

[1] J. Cheng et al. "Isolation of cultured cervical carcinoma cells mixed with peripheral blood cells on a bioelectronic chip," *Analytical Chemistry*, vol. 70, pp.2321-2326, 1998.

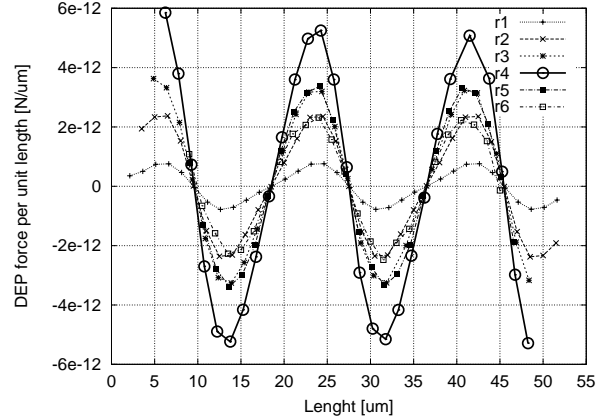


Figure 6: Horizontal DEP forces magnitude per unit length, plotted under the same hypothesis as in fig.5 at a height corresponding to trapping height. The highest DEP force is obtained when $R = l$, where R is the cylinder radius and l is the electrode width.

[2] T. Schnelle et al. "Three-dimensional electric field traps for manipulation of cells - calculation and experimental verification," *Biochimica et Biophysica Acta*, 1157, pp.127-140, 1193

[3] G. Medoro, M. Manaresi, M. Tartagni, R. Guerrieri, "CMOS-only sensor and manipulator for microorganism," *International Electron Devices Meeting*, pp.415-418, 2000

[4] J. Sueheiro and R. Pethig, "The dielectrophoretic movement and positioning of a biological cell using a three-dimensional grid electrode system," *J. Phys. D: Appl. Phys.*, vol. 31, pp. 3298-3305, 1998.

[5] M. P. Hughes, X-B. Wang, J. P. H. Burt, R. Pethig, L. R. Watkins, "Simulations on traveling electric field manipulation of bioparticles," *Computation in Electromagnetic, Second International Conference*, pp.48-51 1994.

[6] H. A. Pohl, "The motion and the precipitation of suspensoids in divergent electric fields," *J. Phys. D: Appl. Phys* , vol. 22, pp.869-874, 1951.

[7] M. Washitzu, T.B. Jones, K.V.I.S. Kaler, "Higher-order dielectrophoretic effects: levitation at field null," *Biochimica et Biophysica Acta*, 1158, pp.40-46, 1993

[8] R.P. Feynman, R.B. Leighton, M. Sands, "Lecture on physics," , vol. II, Addison-Wesley, 1977.

[9] ISE Integrated Systems Engineering AG, "ISE-T-CAD Rel. 5.0."

[10] Arthur R. Von Hippel, "Dielectrics and waves," New York - John Wiley, London - Chapman & Hall, 1954.

[11] Julius Adams Stratton, "Electromagnetic Theory," , Edizioni scientifiche Einaudi, 1952.